This article was downloaded by: [Chalmers University of Technology], [Hans-Georg Scherneck]
On: 04 October 2013, At: 01:25
Publisher: Taylor & Francis
Informa Ltd Registered in England and Wales Registered Number: 1072954 Registered office: Mortimer House, 37-41 Mortimer Street, London W1T 3JH, UK

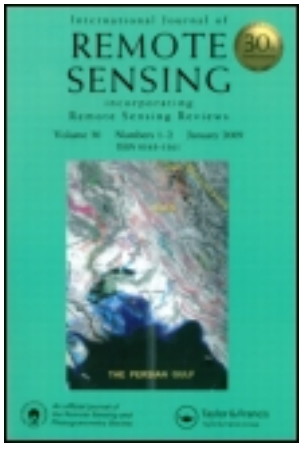

International Journal of Remote Sensing

Publication details, including instructions for authors and subscription information:
http://www.tandfonline.com/loi/tres20

DInSAR investigation in the Pärvie end-glacial fault region, Lapland, Sweden

Matteo Mantovani[a] & Hans-Georg Scherneck[b]

[a] CNR-IRPI, National Research Council - Research Institute for Geo-Hydrological Protection, Padua, Italy

[b] Department of Earth and Space Sciences, CHALMERS University of Technology, Gothenburg, Sweden

To cite this article: Matteo Mantovani & Hans-Georg Scherneck (2013) DInSAR investigation in the Pärvie end-glacial fault region, Lapland, Sweden, International Journal of Remote Sensing, 34:23, 8491-8502

To link to this article: http://dx.doi.org/10.1080/01431161.2013.843871

PLEASE SCROLL DOWN FOR ARTICLE

Taylor & Francis makes every effort to ensure the accuracy of all the information (the "Content") contained in the publications on our platform. However, Taylor & Francis, our agents, and our licensors make no representations or warranties whatsoever as to the accuracy, completeness, or suitability for any purpose of the Content. Any opinions and views expressed in this publication are the opinions and views of the authors, and are not the views of or endorsed by Taylor & Francis. The accuracy of the Content should not be relied upon and should be independently verified with primary sources of information. Taylor and Francis shall not be liable for any losses, actions, claims, proceedings, demands, costs, expenses, damages, and other liabilities whatsoever or howsoever caused arising directly or indirectly in connection with, in relation to or arising out of the use of the Content.

This article may be used for research, teaching, and private study purposes. Any substantial or systematic reproduction, redistribution, reselling, loan, sub-licensing, systematic supply, or distribution in any form to anyone is expressly forbidden. Terms & Conditions of access and use can be found at http://www.tandfonline.com/page/terms-and-conditions

International Journal of Remote Sensing, 2013
Vol. 34, No. 23, 8491–8502, http://dx.doi.org/10.1080/01431161.2013.843871

Taylor & Francis
Taylor & Francis Group

Downloaded by [Chalmers University of Technology], [Hans-Georg Scherneck] at 01:25 04 October 2013

DInSAR investigation in the Pärvie end-glacial fault region, Lapland, Sweden

Matteo Mantovani[a]* and Hans-Georg Scherneck[b]

[a]*CNR-IRPI, National Research Council – Research Institute for Geo-Hydrological Protection, Padua, Italy;* [b]*Department of Earth and Space Sciences, CHALMERS University of Technology, Gothenburg, Sweden*

(*Received 23 April 2013; accepted 19 August 2013*)

Northern Fennoscandia bears witness to the Pleistocene glaciation in the form of a series of large faults that have been shown to have ruptured immediately after the retreat of the ice sheet, about 9500 years ago. The largest one, known as the Pärvie fault, consists of a 155 km long linear series of fault scarps forming north–northeast-trending, that stretch west of Kiruna, Lapland. End-glacial intra-plate faults of this extent are very rare in the continental crust and the Pärvie system represents one of the major fault zone structures of this type in the world. Seismological evidence shows that there is still noticeable seismic activity, roughly one event of magnitude 2 per year that can be attributed to the fault. Nevertheless assessing its state of activity is a difficult task due to the extent and remoteness of the area. This study is aimed at the determination of crustal motion around the Pärvie fault zone using the differential inter-ferometric synthetic aperture radar (DInSAR) technique, based on images acquired with the European Space Agency (ESA) satellites European Remote Sensing (ERS) 1, ERS-2, and the Environmental Satellite (ENVISAT). We present results achieved in terms of deformation of the crystalline bedrock along different sectors of the fault where high levels of coherence were obtained, even from image pairs several years apart. This finding does not exclude deformation in other segments, as observing conditions are not always as favourable in terms of data availability.

1. Introduction

During recession of the latest Pleistocene ice sheet, the ending phase of the Weichselian 9500 years ago, major faults became engaged in Fennoscandia with estimated seismic magnitudes beyond 8 M (Arvidsson 1996). This area is still under-going vertical and horizontal deformation as an effect of glacial isostatic adjustment (GIA), as observed using continuous measurements in the permanent Global Navigation Satellite System (GNSS) networks of the Nordic countries (Johansson et al. 2002; Milne et al. 2004; Lidberg et al. 2010). It appears that the faults respond to ongoing stress changes, and it is suggested that they might accumulate a part of the post-glacial rebound strain in their environment. Signs of persistent weakness are found in a higher-than-average contemporary seismicity as noted by e.g. Miur Wood (1993). End- or post-glacial intra-plate structures of this extent are very rare in the continental crust. One may argue that due to young age of the faults, the conditions on the fault plane at depth could still be affected by the heat release during the major

*Corresponding author. Email: matteo.mantovani@irpi.cnr.it

© 2013 Taylor & Francis

shock, making the fault zone admissible to enhanced creep as compared to the regular lithosphere sections. The fact that the traces and heights of the individual segments belonging to a certain fault set, as well as the gaps in between the separate sections, appear to be largely governed by the structures and composition of the superficial bedrock indicates that more continuous faulting and rupture must occur at depth.

Pärvie is the largest fault system in Fennoscandia, and assessing its deformations is well motivated with reference to its spatial extent and its present seismicity. The fault structure is on a spatial scale that is difficult to resolve with the ∼200 km mesh width GNSS network, and other direct measurements of its state of activity in terms of crustal deformation (displacement rates, strain rates) do not yet exist. In this remote area, in fact, measurement that involves ground-based instrumentation is difficult. We used the differential interferometric synthetic aperture radar (DInSAR) technique to detect and measure deformations, since it offers the possibility to measure displacements at centimetre to millimetre accuracy over long time periods in large inaccessible areas, coupling the precision of geodetic surveys with the advantages of remote-sensing techniques. Seventy-two European Remote Sensing (ERS) images of two different descending orbits and 12 Environmental Satellite (ENVISAT) acquisitions covering a time span of 17 years (1992–2009) were processed. Fringes attributed to crustal deformations have been detected over short segments in the northern part of the Pärvie fault zone.

2. Late Quaternary faults in northern Fennoscandia

Large fault systems that can be attributed to ice sheet loading and unloading appear to be a rare phenomenon on the Earth. In northern Fennoscandia, we know of nine separate fault structures with mapped scarp lengths at or exceeding 10 km, notably Pärvie (150 km), Stouragurra (80 km), Lainio-Sujavaara (50 km), Suasselkä (48 km), Lansjärv (40 km), Burträsk (40 km), Skellefteå (30 km), and Pasmajärvi–Venejärvi (15 km), see Lagerbäck (1978), Olesen (1988), and Kujansuu (1964) (Figure 1).

That their activation coincides with the receding of the Weichsel glaciation's ice sheet is supported by Quaternary geological research (Lagerbäck and Sundh 2008). Less clear is whether they were either created or re-activated in the most recent deglaciation. The fault systems nearly always follow pre-existent fracture patterns (Munier and Fenton 2004). Stress accumulation may have extended existing fault planes and brought some of them into connection. In no cases are the fault systems correlated with boundaries of geological complexes or tectonic units, not even rock type. The transition from the situation when the crust was charged by an order of magnitude 1 km thick ice sheet to a completely load-free situation caused significant change of the state of stress in the crust, favouring failure predominantly in the early phase of the unloaded state. Activation may have been a direct response to ambient stress exceeding fault stability limits and fractural strength, or a combined effect of stress and a weakening process, for instance increase of hydrostatic pore pressure in rock volumes with favourable porosity and permeability (Lund 2005; Lund, Schmidt, and Hieronymus 2009). Particularly important with respect to our investigation is the character of the stress field that Lund (2005) predicts for the present day. The models for deviatoric background stress show persistence of a stress character that favours a reverse faulting style while the magnitude of the load-induced deviatoric stress is relaxing. Regarding nomenclature, among the alternative designations late Quaternary, post-glacial, or end-glacial for the Pärvie fault, we choose end-glacial, since at least some segments of it were ice-covered at the point of activation (Lagerbäck 1978).

Downloaded by [Chalmers University of Technology], [Hans-Georg Scherneck] at 01:25 04 October 2013

Downloaded by [Chalmers University of Technology], [Hans-Georg Scherneck] at 01:25 04 October 2013

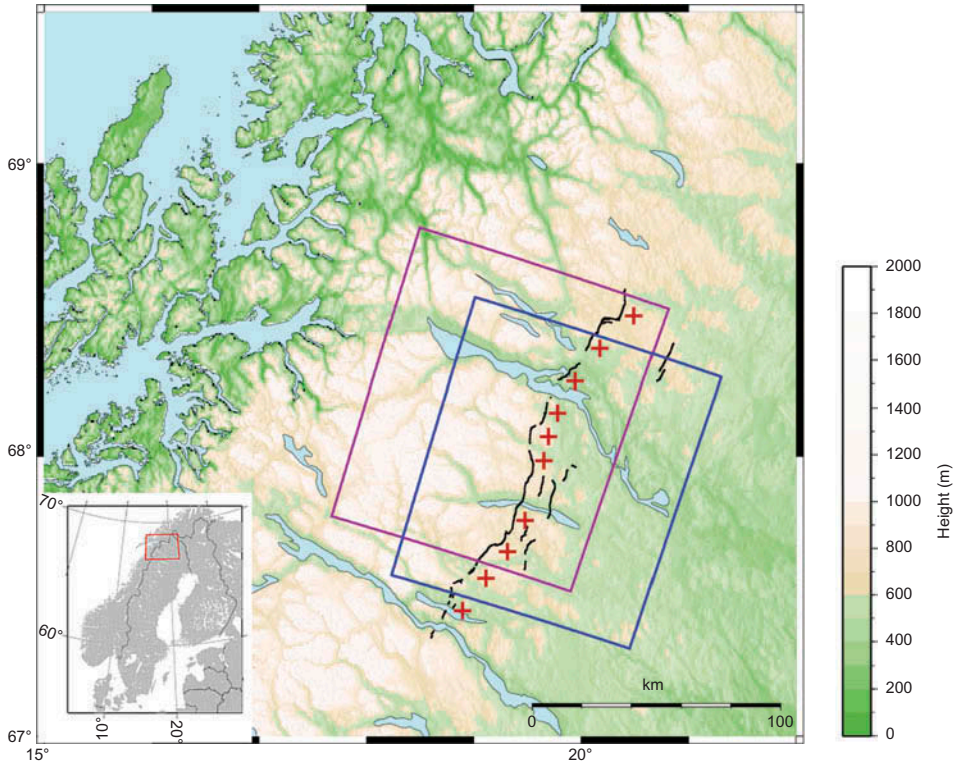

Figure 1. The Pärvie fault system (black lines). Red plus symbols indicate the uplifted blocks while blue and purple squares represent the perimeters of track 480-frame 2223 and track 251-frame 2223 SAR scenes, respectively. Latitudes are due north and longitudes due east. The colour coding of land elevation emphasizes that the tree line in the area of the fault zone runs near 500 m above sea level.

The faults are found in old bedrock. The part of the Baltic shield formed in the mid-Paleozoic (1.96–1.87 Ga) in the Svekokarelian orogeny. A period of strike-slip megashear followed (Berthelsen and Marker 1986). Latest magmatic events, dike intrusions, are dated to 1.1 Ga or older. Fracture zones with strikes along NW–SE and N–S have been pointed out by Henkel (1989) to possibly be related to the generation of the dikes. Later on, Caledonian nappes covered a wide area to the east of the mountain chain starting in the Early Devonian, 407 Ma. Denudation of this cover ended in the Tertiary. The Pärvie fault runs merely clear of the Caledonian thrusts remains; in the south, it appears to end at the Caledonian front line.

3. Pärvie fault system

The main Pärvie system consists of a linear series of scarps, almost all of them west-facing and together forming a north–northeast-trending, 155 km long fault line. Only in a lesser part of its stretch does the fault appear to fan out towards the surface to create parallel escarpments. At varying distances to the east of the master fault, there are a number of subsidiary scarps, almost all of them east-facing, i.e. opposite to the master. The birth (alternately, the most recent re-activation) of the Pärvie fault system is rather well dated at 9500 BP (Lagerbäck 1992). Some segments had still been covered with ice.

Figure 2. Aerial view of the Pärvie fault scarp acquired from coordinates 19.54482° E, 67.95022° N, height 300 m above ground and looking to the northeast (photograph by Hans-Georg Scherneck).

Its faulting is associated with an earthquake; Arvidsson (1996) estimated the earthquake moment magnitude at 8.2 ± 0.2, assuming that the Pärvie ruptured the whole crust along the entire fault length in a single event. Several morphological features, for instance the occurrence of melt-water channels cutting the fault scarp, have confirmed this assumption; yet, examination by trenching has not been carried out across these scarps (Lundqvist and Lagerbäck 1976; Lagerbäck and Witschard 1983; Lagerbäck 1990, 1992; Miur Wood 1993). Bedrock exposures occur rather frequently, and at several locations, overhanging cliffs indicate reverse movement on steeply dipping fault planes (near 50°). This is in itself unusual in tectonics, as steeply dipping fault planes are commonly associated with normal, not reverse fault slip. Field observation and photogrammetric measurements indicate that fault scarp heights generally vary between 3 and 10 m (Figure 2), but locally somewhat greater heights were measured (Lagerbäck and Sundh 2008; Lagerbäck and Witschard 1983).

4. Seismicity

Signs of persistent weakness are found in a higher-than-average contemporary seismicity as noted by e.g. Miur Wood (1993). The Swedish National Seismic Network (SNSN) has, since its extension into Lapland in the year 2000, regularly been observing earthquakes at or even below the magnitude-0 level (Bödvarsson and Lund 2003). The distribution of magnitude *versus* frequency is such that typically one 3 Mw event occurs in a 10 year time span. Arvidsson (1996) suggests that 50% of the seismicity in Northern Sweden (66° N) is associated with the end- or post-glacial faults. Recently, Lindblom et al. (2011) and Lindblom and Lund (2011) used regional micro-earthquakes that are probably occurring on the Pärvie fault planes (but in part also on secondary faults), possibly to be seen as late aftershocks, to map the fault plane at greater depth (down to 30 km) and also to examine the fault mechanisms. From the south to the centre, the fault mechanism starts from being mostly reverse to gradually gain a strike-slip component. The pattern repeats on the way north, and it appears as if the strike-slip segments correlate with the two valleys (Nikkaluokta and Torneträsk). A few normal-faulting events have been identified. While in single cases the sources may be located on crossing subsidiary faults on which the stress regimes are opposite to the

Downloaded by [Chalmers University of Technology], [Hans-Georg Scherneck] at 01:25 04 October 2013

Downloaded by [Chalmers University of Technology], [Hans-Georg Scherneck] at 01:25 04 October 2013

conditions in the main fault, a compressive stress regime appears to dominate the overall pattern. Lindblom and Lund (2011) go on in their study to show the compatibility of this stress regime with ongoing GIA (post-glacial land uplift) in Fennoscandia. They reduce the problem to one fault being exposed to a purely compressive stress regime. Given the episodic nature of seismic event sequences, we expect displacements in the fault system to average over time and space to values below 1 mm year^{-1}, more probably only at 0.1 mm year^{-1}.

5. Observations of deformation due to GIA in Fennoscandia

More direct evidence for crustal deformation may be found in space-geodetic investigations using GNSS, in particular the Global Positioning System (GPS) due to its availability since the late 1980s. In this technique, the geodetic position of permanently installed and continuously operating GNSS (CGNSS) receivers are estimated from dual-frequency phase-measurements, and station velocity vectors are inferred from multi-year time series analysis comprising thousands of daily position estimates after mapping the regional network into the International Terrestrial Reference Frame (ITRF). The Baseline Inferences on Fennoscandian Rebound Observations, Sealevel and Tectonics (BIFROST) project was launched in 1992 for the purpose of investigating the effects of GIA in Fennoscandia, including inference of sea-level variations and tectonics. We refer to Lidberg et al. (2010) for the hitherto most comprehensive analysis of GNSS observations in Fennoscandia with regard to both temporal and spatial extent. One study that attempted to analyse the velocity field obtained from the BIFROST project in terms of strain and curl with a slight potential of discerning regional patterns, however only on a special scale greater than 200 km, was presented in Scherneck et al. (2010). In this work, the Lapland region indeed exhibited a few peculiar features. The error analysis suggests that strain rates could be determined at the 2 nano year^{-1} and curl at the 0.5 nrad year^{-1} level. An order-of-magnitude estimate yields a 95% confidence detection threshold

$$V_{thr} \approx 3 \times 100 \text{ km} \times 10^{6} \text{ mm km}^{-1} \times 2 \times 10^{-9} \text{ year}^{-1} \approx 0.6 \text{ mm year}^{-1}, \quad (1)$$

for expected displacement rate over 100 km, the length scale of the fault.

6. DInSAR analysis

DInSAR analysis represents one of most recognized and well-established techniques for detection and measurement of crustal deformations. Since one of the first and probably the most famous application on the Landers earthquake (Massonnet et al. 1993), DInSAR has been applied to all the other forms of surface deformation processes, such as volcanism, subsidence, and landslides. Since then, advanced DInSAR techniques have been developed to overcome some of the limitations of the original approach and to provide better results in terms of accuracy, reliability, and robustness of the deformation measurements, exploiting large amounts of data. Among these, we emphasize the permanent scatterer (PS) technique developed by Ferretti, Prati, and Rocca (2000) and the short baselines subsets (SBAS) approach used by Berardino et al. (2002). The theory and principles of DInSAR is beyond the scope of this article, and for a comprehensive overview of the interferometric techniques, it is suggested to refer to Raucoules, Colesanti, and Carnec (2007). In this study, we exploited European Space Agency (ESA) satellites ERS-1, ERS-2, and ENVISAT data archives, which to present time, are the most complete and long series of SAR images

Downloaded by [Chalmers University of Technology], [Hans-Georg Scherneck] at 01:25 04 October 2013

covering the area of interest. Application to the boreal landscape contains a number of complications and obstacles.

Lapland is characterized by boreal forest and tundra, but in parts it is also completely barren. Vegetation is classified as alpine (barren) to northern boreal. Bedrock exposures, eventually fragmented to rubble at the surface, occur rather frequently along parts of the fault, surface properties which in illumination with radar favour the preservation of the coherence between images acquired years apart. Since deformation expected along the fault are thought in terms of millimetres or less per year as inferred from the previous analysis, the conditions for applying DInSAR with long series of SAR scenes appeared promising. However, yet expectedly, snow-free conditions prevail generally for only two to three months per year due to the long winter, which limits the data usability. With the images at our disposal, we have been able to frame more than 120 km of the Pärvie fault, that is 80% of its length.

The fault was divided into seven segments that were analysed separately for computational reasons but also because in this way we were able to consider the glacial isostatic uplift as a constant bias within each frame. Seventy-two descending-track acquisitions from ERS (track 251-frame 2223 and track 480-frame 2223) and 12 from ENVISAT (track 251-frame 2223) covering a time span of 17 years (1992–2009) were selected. A 50 m resolution digital elevation model (DEM), with a height accuracy of 2 m, was oversampled by a factor of 2, both in range and azimuth, to obtain a 25 m resolution cell and it was used to generate the synthetic interferogram, which allowed us to remove the phase term related to the topography. The original data is based on photogrammetric analysis of aerial stereo photography taken at the end of the 1970s and it is not likely possible that the topography of the area of interest changed significantly from the date of acquisition until the period of investigation. The fault is well recognizable in the filtered amplitude images and in the superimposed synthetic interferogram as shown in in Figure 3.

Since the data set is too poorly sampled over time for the advanced DInSAR techniques, a conventional analysis was carried out. We selected those images that showed the most promising correlation and the most suitable (i.e. the shortest) baselines, since these will help to suppress DEM errors. More than 100 differential interferograms with a perpendicular baseline smaller than 150 m were generated after the adjustment of the orbits, using the

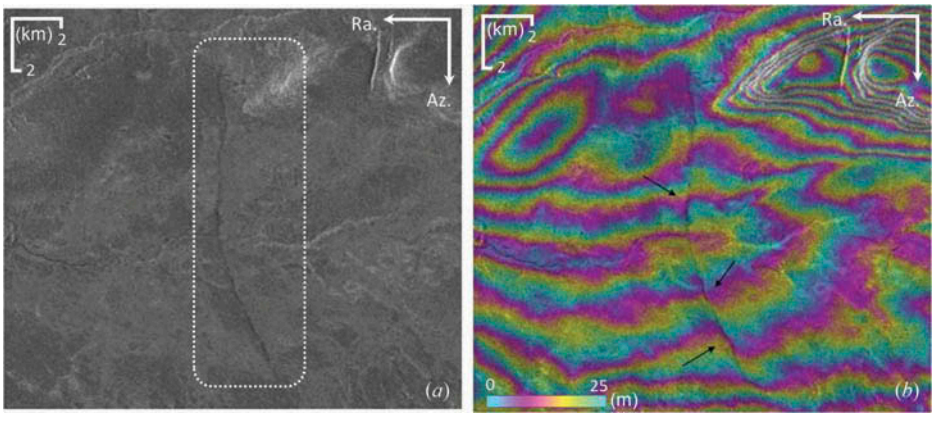

Figure 3. Amplitude image (*a*) and synthetic interferogram (*b*) of the central sector of the Pärvie fault (centre of the image 19.53168° E, 67.97204° N). The scarp is highlighted by a white rectangle (*a*) and black arrows (*b*).

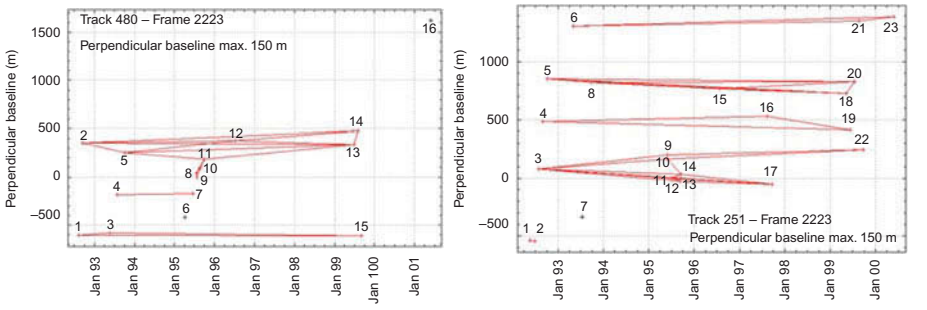

Figure 4. Connection graphs for ERS track 480 and 251 datasets with a perpendicular baseline upper constraint of 150 m.

precise ephemeris that Delft University had made available on their website (http://www.deos.tudelft.nl/ers/precorbs/orbits), and after the subtraction of the topographic phase term. Despite the large amount of data at our disposal, the actual number of suitable interferograms was too poor to apply advanced DInSAR techniques (see Figure 4). We processed data acquired in snow-free or almost snow-free conditions (from late May to the beginning of October) and discarded 23 images taken after the ERS-2 gyroscope's failure (February 2001). The interfero-metric analysis was hence conducted for 16 ERS track-480 acquisitions, 23 ERS, and 8 ENVISAT track-251 images. Among these, we considered only acquisitions with a perpendicular baseline up to 150 m. Considering the DEM height accuracy, the smooth topography of the area investigated, and an altitude of ambiguity of at least 60 m, given our baseline constraint for useful data sets, we were able to efficiently suppress the phase term related to DEM errors. More than 60 differential interferograms were generated after the adjustment of the orbits, using the precise ephemeris that Delft University had made available on their web site (http://www.deos.tudelft.nl/ers/precorbs/orbits). A minimum-cost flow algorithm was used to unwrap the phase, and areas with a coherence less than 0.6 were masked out. Since, in single interferograms, delay patterns due to radiation propagation in heterogeneous (wet) atmosphere can be confused with deformation fringes, we used a qualitative approach to assess the state of activity of the fault by simply comparing the phase images generated from independent data. The properties of interferograms presented in this study, where deformation-related patterns have been detected, are summarized in Table 1.

Table 1. Characterstics of the interferograms.

INT. (n°)	Data set (mission)	Master (yyyy-mm-dd)	Slave (yyyy-mm-dd)	ΔBaseline* (days)	⊥Baseline† (m)	ALT. of AMB (m)
1	ERS-480	1992-09-17	1996-07-07	1389	27	344
2	ERS-480	1992-09-17	1999-06-27	2474	−16	581
3	ERS-480	1993-07-29	1994-06-17	688	16	581
4	ERS-480	1996-07-07	1999-06-27	1085	44	211
5	ERS-251	1992-07-28	1995-07-06	1073	−76	122
6	ERS-251	1995-07-07	1997-09-19	805	53	175
7	ENVISAT-251	2004-08-13	2007-08-03	1085	148	63
8	ENVISAT-251	2005-07-29	2007-09-07	770	77	120
9	ENVISAT-251	2007-08-23	2009-08-07	735	−88	105

Notes: *Temporal baseline.
†Perpendicular baseline.

Downloaded by [Chalmers University of Technology], [Hans-Georg Scherneck] at 01:25 04 October 2013

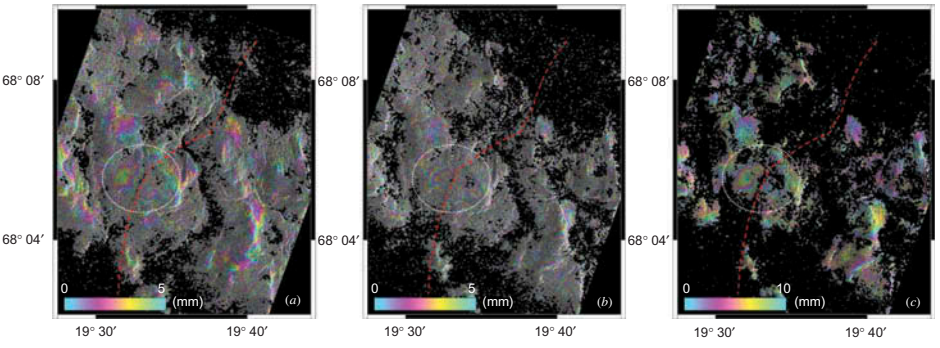

Figure 5. Differential interferograms generated from ERS track 480 images: 17 September 1992 and 7 July 1996 (*a*); 7 July 1996 and 27 June 1999 (*b*); 17 September 1992 and 27 June 1999 (*c*). The red line represents the segments of the Pärvie fault; the dotted white ellipse highlights the deformation area. Note that one colour cycle corresponds to 10 mm of LOS deformation in interferogram (*c*) and 5 mm in others (*a*, *b*).

We have been able to identify small displacements over three segments in the northern sectors of the fault. The most evident cases were recorded in the area between the lakes Nakerjaure and Kuolasjavre (lat. 68.0958°; long. 19.5189°). Despite atmospheric disturbances, a pattern of deformation is clearly visible near the major fault in all the interferograms produced from three images acquired from track 480 (Figure 5).

The increment of the deformation with time, which can be noticed from Figure 5, provides further confidence of a crustal deformation process being present. Interferogram analysis showed that displacements are higher between the years 1996–1999 than 1992–1996. Knowing that we are able to detect just the component of the deformation along the line of sight (LOS) of the radar, which has a slope of about 23° with respect to the local vertical, we can assert that the right hand side of the fault moved towards the sensor relatively to the left side. Interferograms are, in fact, displayed in range-doppler coordinates and, since they have been acquired from descending orbits, the geographic east is on the left while the west is on the right of the images; they are also slightly rotated counterclockwise with respect to the north. Additional confirmation of the activity of this sector is provided comparing the former interferograms with those generated from data sets acquired by ERS and ENVISAT satellites along track 251 (Figure 6).

The most recent interferogram (Figure 6(*c*)) recorded the highest displacement over the area. The estimated rate of deformation is about 5 mm year^{-1}, which is roughly double that of those assessed from the previous interferograms. The second area subjected to deformation was detected between the lakes Kuolasjaure and Laukujarvi (67.9237° N; 19.6602° E). Figure 7 shows the interferograms produced by the three independent data sets. Rates of deformations along the LOS, measured by ERS data sets, are quite similar ranging from 3 to 4 mm year^{-1}, while higher displacements are recoded, once again, by the more recent ENVI interferogram with 7 mm year^{-1}. Contrarily to the former case, along this sector of the fault, the area moved away from the sensor relative to the surroundings.

Fringes related to deformation were also detected in the northernmost sector of the fault, close to the border between Norway and Sweden (lat. 68.4299°; long. 20.2048°). Since this area was not covered by track 480, confrontations were made among two independent interferograms for each track 251, ERS, and ENVISAT data set (Figure 8).

Downloaded by [Chalmers University of Technology], [Hans-Georg Scherneck] at 01:25 04 October 2013

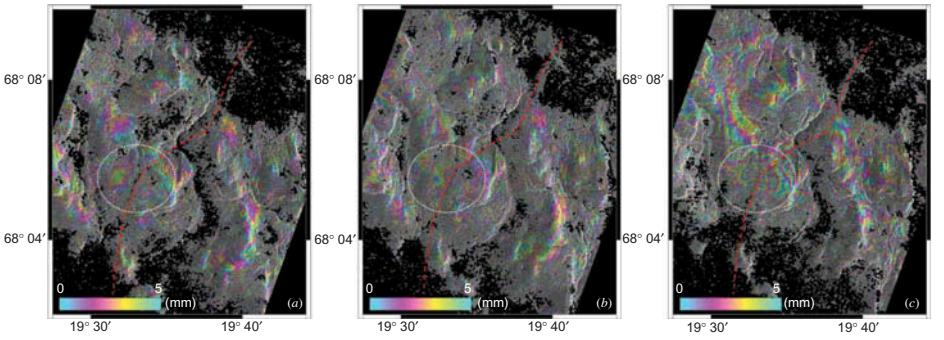

Figure 6. Differential interferograms generated from images: 17 September 1992 and 7 July 1996, ERS track 480 (*a*); 28 July 1992 and 6 June 1995, ERS track 251 (*b*); 3 August 2007 and 7 August 2009, ENVISAT track 251 (*c*). The red line represents the segments of the Pärvie fault; the dotted white ellipse highlights the deformation area.

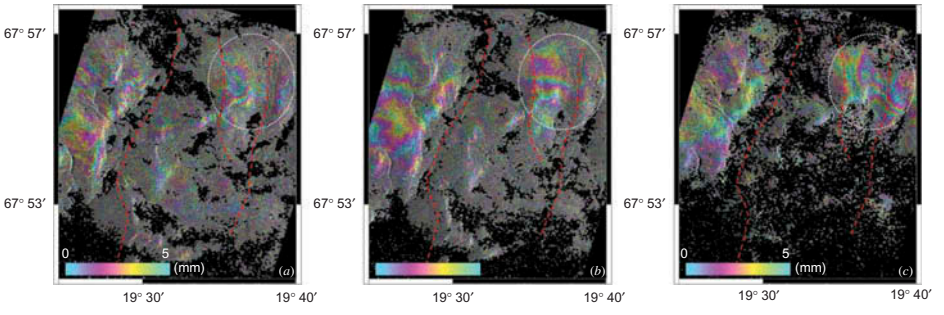

Figure 7. Differential interferograms generated from images: 29 July 1993 and 17 June 1995, ERS track 480 (*a*); 7 July 1995 and 19 September 1997, ERS track 251 (*b*); 3 August 2007 and 7 August 2009, ENVISAT track 251 (*c*). The red line represents the segments of the Pärvie fault; the dotted white ellipse highlights the deformation area.

From the interferograms, we can infer that the area on the left hand side of the fault (geographical East) moved closer to the radar with respect to the right hand side (geographical West), with a maximum rate of about 2–3 mm year^{-1}, which can be considered constant in all the four interferograms.

7. Discussion

A conventional DInSAR analysis bears more errors in the assessment of the deformations compared to advanced techniques. It is not just the accuracy of the measurements that is poorer but even the detection of the displacements can be misinterpreted, since a range of different signatures in the interferograms may wrongly be attributed to ground deformations. Candidates among these signatures are different propagation times of the illuminating radiation through the ionosphere and troposphere layers that, between two acquisitions, lead to phase variations similar to those generated by the surface deformation processes; others are residual orbital components and uncompensated topography generates phase shifts that are not always negligible. Since ground deformations in the same locations are expected to be temporally correlated and atmospheric artefacts are not, they hence can be discriminated using independent interferograms (Raucoules, Colesanti, and Carnec 2007). We can assert

Downloaded by [Chalmers University of Technology], [Hans-Georg Scherneck] at 01:25 04 October 2013

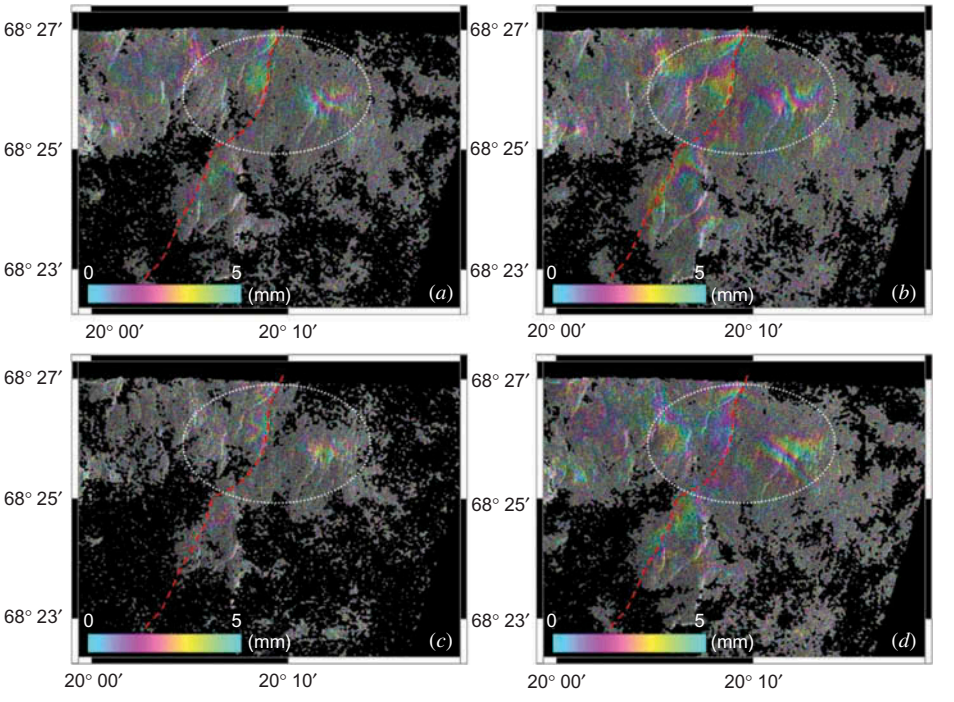

Figure 8. Differential interferograms generated from ERS track 251 images: 28 July 1992 and 6 July 1995 (*a*); 7 July 1995 and 19 September 1997 (*b*); and from ENVISAT track 251 acquisitions: 13 August 2004 and 3 August 2007 (*c*); 29 July 2005 and 7 September 2007 (*d*). The red line represents the segments of the Pärvie fault; the dotted white ellipse highlights the deformation area.

that fringe patterns recorded at three different locations of the Pärvie fault are certainly related to deformation because they are consistent not only among several interferograms that do not share a common image, but also among data sets acquired by different sensors. Moreover, the sources of errors that affect the phase measurements have been reduced through the use of corrected orbital parameters, small baseline pairs, and a high quality DEM. Still, the rate of deformation measured in the interferogram is affected by an error due to the atmospheric phase delay that was not removed or modelled. To sum up, what can be reasonably inferred after the DInSAR analysis is that three short sections of the Pärvie fault are active, and the component of the deformation along the LOS is quantifiable in a few millimetres per year. We can also assume that the displacements occurred mainly along the vertical direction, indicating a reverse slip mechanisms. The latter statement comes from the following geometrical considerations. SAR images were acquired along a track with a heading angle between –161° and –162°. As the fault is orientated with an angle of approximately between 15° and 25° East from North, the scarps run practically parallel to the satellites' orbit. Considering that the sensitivity versor (Massonnet and Feigl 1998) is equal to

$$\bar{u} = \begin{bmatrix} u_{\mathrm{East}} \\ u_{\mathrm{North}} \\ u_{\mathrm{Zenith}} \end{bmatrix} \approx \begin{bmatrix} 0.373 \\ -0.124 \\ 0.919 \end{bmatrix}, \tag{2}$$

and that the system has no sensitivity along the sensor trajectory, we can infer that the along fault motion is zero. If there were cross-fault motion, the displacements would be too large

Downloaded by [Chalmers University of Technology], [Hans-Georg Scherneck] at 01:25 04 October 2013

to be admissible (more than 13 mm year^{-1}) and hence we can assume that the deformation has occurred mainly along the vertical direction.

8. Conclusions

Retrieving displacements that, if they exist, are in the order of a few millimetres or less per year in boreal regions is not an easy task. Signal decorrelation due to the persistent presence of snow on the ground together with total absence of man-made structures strongly reduces the application of advanced interferometric techniques such as PS or SBAS. As of the present, DInSAR appears to be the only approach that can be used to assess the state of activity of the Pärvie. Despite numerous limiting factors, some promising results have been achieved. We were able to detect patterns of deformations along different segments of the fault that are consistent with the predominantly reverse-slip mechanisms proposed by Lindblom et al. (2011) and Lindblom and Lund (2011); however, in the specific geometry of fault *versus* satellite orbit, the interferometric analysis cannot confirm the strike-slip mechanisms. Examining interferometric fringes in the radar imagery, we detect consistent patterns of deformation in independent data sets. Displacement increases with time, thus the notion of deformation rate applies. By the same token, a notion of episodic character appears unlikely. Thus, we propose that a persistent source of stress is in action that, combined with lower strength of the crust in the fault zone region, leads to enhanced creep compared to regular lithosphere sections. Finally, DInSAR analysis contributed to enlarge the observational database of contemporary measurement of GIA in a global perspective, providing relevant information otherwise impossible to collect. Our findings contribute to the pre-studies of the DAFNE post-glacial fault drilling project, and we are looking forward to a range of ensuing *in situ* investigations to bring clarity as to the prevailing state of stress in this mega-fault complex.

Acknowledgements

This work has been carried out under the LaFaZONES project, supported by the Swedish National Space Board (contract n. 112/09: 1). The authors acknowledge the European Space Agency for providing ERS and ENVISAT data (C1P.7559). SAR processing was performed using Gamma Software (GAMMA Remote Sensing Research and Consulting AG, Gümligen, Switzerland). We thank Odleiv Olesen for critical comments and for bringing reference material to our attention. We thank two anonymous reviewers for their significant comments that helped improve the manuscript.

References

Arvidsson, R. 1996. "Fennoscandian Earthquakes: Whole Crustal Rupturing Related to Post-Glacial Rebound." *Science* 274: 744–746.

Berardino, P., G. Fornaro, R. Lanari, and E. Sansosti. 2002. "A New Algorithm for Surface Deformation Monitoring Based on Small Baseline Differential SAR Interferograms." *IEEE Transactions on Geoscience and Remote Sensing* 40: 2375–2383.

Berthelsen, A., and M. Marker. 1986. "1.9–1.8 Ga Old Strike–slip Megashears in the Baltic Shield, and Their Plate Tectonic Implications." *Tectonophysics* 128 (3–4): 163–181.

Bödvarsson, R., and B. Lund. 2003. "The SIL Seismological Data Acquisition System as Operated in Iceland and Sweden." In *Methods and Application of Signal Processing in Seismic Network Operations. Lecture Notes in Earth Sciences No. 98,* edited by T. Takanami, and G. T. Kitagawa, 131–148. Berlin: Springer Verlag.

Ferretti, A., C. Prati, and F. Rocca. 2000. "Nonlinear Subsidence Rate Estimation Using Permanent Scatterers in Differential SAR Interferometry." *IEEE Transactions on Geoscience and Remote Sensing* 38: 2202–2212.

Downloaded by [Chalmers University of Technology], [Hans-Georg Scherneck] at 01:25 04 October 2013

Henkel, H. 1989. "Tectonic Studies in the Lansjärv Region." In *Interdisciplinary Study of Post-Glacial Faulting in the Lansjärv Area, Northern Sweden, 1996–1998. Technical Report TR-89-31,* edited by G. Bäckblom and R. Stanfors. Stockholm: SKB, Swedish Nuclear Fuel and Waste Management.

Johansson, J. M., J. L. Davis, H.-G. Scherneck, G. A. Milne, M. Vermeer, J. X. Mitrovica, R. A. Bennett, B. Jonsson, G. Elgered, P. Elósegui, H. Koivula, M. Poutanen, B. O. Rönnäng, and I. I. Shapiro. 2002. "Continuous GPS Measurements of Postglacial Adjustment in Fennoscandia 1. Geodetic Results." *Journal of Geophysical Research* 107 (B8). doi:10.1029/2001JB000400

Kujansuu, R. 1964. "Nuorista siirroksista Lapissa (Recent Faulting in Lapland)." *Geologi* 16: 30–36.

Lagerbäck, R. 1978. "Neotectonic Structures in Northern Sweden." *Geologiska Föreningens T Stockholm Förhandlingar* 100: 263–269.

Lagerbäck, R. 1990. "Late Quaternary Faulting and Paleoseismicity in Northern Fennoscandia, with Particular Reference to the Lansjärv Area, Northern Sweden." *Geologiska Föreningens T Stockholm Förhandlingar* 112: 333–354.

Lagerbäck, R. 1992. "Dating of Late Quaternary Faulting in Northern Sweden." *Journal of Geological Society, London* 149: 285–291.

Lagerbäck, R., and M. Sundh. 2008. *Early Holocene Faulting and Paleoseismicity in Northern Sweden. Tech. Rep. C 836*. Uppsala: SGU, Geological Survey of Sweden, Research Paper.

Lagerbäck, R., and F. Witschard. 1983. *Neotectonics in Northern Sweden Geological Investigations. Tech. Rep. TR-83-58*. Stockholm: SKB, Swedish Nuclear Fuel and Waste Management.

Lidberg, M., J. M. Johansson, H.-G. Scherneck, and G. A. Milne. 2010. "Recent Results Based on Continuous GPS Observations of the GIA Process in Fennoscandia from BIFROST." *Journal of Geodynamics* 50: 8–18.

Lindblom, E., and B. Lund. 2011. "Focal Mechanisms and the State of Stress Among the Pärvie End-Glacial Fault, Northern Sweden." Paper II in Lic. thesis., Uppsala Universitet, Department of Earth Sciences.

Lindblom, E., B. Lund, A. Tryggvason, M. Uski, C. Juhlin, R. Bödvarsson, and R. Roberts. 2011. "Microearthquake Activity on the Pärvie End-Glacial Fault System, Northern Sweden." Paper I in Lic. thesis., Uppsala Universitet, Department of Earth Sciences.

Lund, B. 2005. *Effects of Deglaciation on the Crustal Stress Field and Implications for Endglacial Faulting: A Parametric Study of Simple Earth and Ice Models. Tech. Rep. TR-05-04*. Stockholm: SKB, Swedish Nuclear Fuel and Waste Management.

Lund, B., P. Schmidt, and C. Hieronymus. 2009. *Stress Evolution and Fault Stability During the Weichselian Glacial Cycle. Tech. Rep. TR-09-15*. Stockholm: SKB, Swedish Nuclear Fuel and Waste Management.

Lundqvist, J., and R. Lagerbäck. 1976. "The Pärvie Fault: A Late-glacial Fault in the Precambrian of Swedish Lapland." *Geologiska Föreningers T Stockholm Förhandlingar* 98: 45–51.

Massonnet, D., and K. L. Feigl. 1998. "Radar Interferometry and Its Application to Changes in the Earth's Surface." *Reviews of Geophysics* 36: 441–500.

Massonnet, D., M. Rossi, C. Carmona, F. Adragna, G. Peltzer, K. Feigl, and T. Rabaute. 1993. "The Displacement Field of the Landers Earthquake Mapped by Radar Interferometry." *Nature* 364: 138–142.

Milne, G. A., J. X. Mitrovica, H.-G. Scherneck, J. L. Davis, J. M. Johansson, H. Koivula, and M. Vermeer. 2004. "Continuous GPS Measurements of Postglacial Adjustment in Fennoscandia: 2. Modeling Results." *Journal of Geophysical Research* 109: B02412.

Miur Wood, R. 1993. *A Review of the Seismotectonics of Sweden. Tech. Rep. TR-93-13*. Stockholm: SKB, Swedish Nuclear Fuel and Waste Management.

Munier, R., and C. Fenton. 2004. *Review of Postglacial Faulting. Tech. Rep. R-04-17, App. 3*. Stockholm: SKB, Swedish Nuclear Fuel and Waste Management.

Olesen, O. 1988. "The Stuoragurra Fault; Evidence of Neotectonics in the Precambrian of Finnmark, Northern Norway." *Norsk Geologisk Tidsskrift* 68: 107–118.

Raucoules, D., C. Colesanti, and C. Carnec. 2007. "Use of SAR Interferometry for Detecting and Assessing Ground Subsidence." *Comptes Rendus Geoscience* 339: 289–302.

Scherneck, H.-G., M. Lidberg, R. Haas, J. M. Johansson, and G. A. Milne. 2010. "Fennoscandian Strain Rates from BIFROST GPS: A Gravitating Thick-Plate Approach." *Journal of Geodynamics* 50: 16–19.

Downloaded by [Chalmers University of Technology], [Hans-Georg Scherneck] at 01:25 04 October 2013